Crystalline, Ordered and Disordered Lipid Membranes: Convergence of Stress Profiles due to Ergosterol

Juan M. Vanegas,[†] Marjorie L. Longo,[†,‡] and Roland Faller*,[†,‡]

[†]Biophysics Graduate Group and [‡]Chemical Engineering and Materials Science Department, University of California, Davis, California 95616, United States

S *Supporting Information*

ABSTRACT: We present a simulation study focusing on modulations of the stress, or lateral pressure, profiles of lipid bilayer phases by addition of a sterol, ergosterol, at multiple temperatures. A major redistribution of lateral and normal pressures across the gel-phase bilayer required 10 mol % sterol in comparison to a gradual redistribution beginning at 20 mol % for the liquid phase. Stress profiles across all temperatures converged at 30 mol % ergosterol. Redistribution and merging of stress profiles, associated with structural alterations, are coincident with experimentally observed modulations in mechanical properties and therefore are suggested as the mechanism of action for this biologically necessary role of sterols.

L ipid membranes are nature's way to compartmentalize cells from their environments as well as organize and regulate the complex processes taking place within them. Two major components of cell membranes are phospholipids, e.g., phosphatidyl choline (PC) and sterols.[1] For unicellular organisms, such as yeasts, ergosterol is the sterol of choice and is present in their membranes anywhere from ~10 to ~30 mol %.[2,3] Yeasts have broad technological use, and a mechanistic understanding of ergosterol's role in membrane behavior is important.[4] The phase behavior of lipid bilayers is significantly controlled by sterol content enabling the so-called liquid-ordered phase in addition to the gel and fluid phases.[5] It is believed that "rafts" in cell membranes are induced by the liquid-ordered phase.[6] While it is still debated whether ergosterol-containing membranes form "rafts", new evidence may support this idea.[7,8]

In this work we focus on the membrane stress, or lateral pressure, profile which has in recent years gained significant interest.[9–15] This is in part due to the connection between the stress profile and bilayer mechanical properties,[16] and potential modulation of membrane protein function.[11] The stress profile $\pi(z)$ is obtained from the diagonal elements of the local pressure tensor $\mathbf{P}(\mathbf{r})$ averaged over the membrane plane: $\pi(z) = (P_{xx} + P_{yy})/2 - P_{zz}$. The local pressure tensor can be expressed in terms of an "energy density" with a kinetic and configurational component, and is obtained from the positions and velocities of the atoms:

$$\mathbf{P}(\mathbf{r}) = \sum_i m_i \mathbf{v}_i \otimes \mathbf{v}_i + \frac{1}{V} \sum_{i<j} \mathbf{F}_{ij} \otimes \mathbf{r}_{ij}$$

Although currently there are no experimental methods to directly obtain the stress profile of a membrane, experimentally relevant elastic properties such as the area compressibility and bending moduli can be directly obtained from the stress profile.[16] In general, negative values in the stress profile contribute toward membrane contraction, while positive values favor expansion. Stress profiles provide important details of favorable and unfavorable interactions across a membrane, which may aid in the understanding of protein function, phase behavior, and small-molecule transport.

Previous molecular dynamics simulation studies of stress profiles have focused on fluid-phase membranes (containing unsaturated lipids or at high temperatures), with only one coarse-grained study[9] briefly addressing the gel phase. To the best of our knowledge stress profiles have never been used to identify differences between gel and liquid phases or the transition between the gel and liquid-ordered phase at the atomistic simulation level. This may stem from the significant computational cost involved in simulating gel phase membranes which have 10–20 times slower dynamics. It is not clear how the transition from the two potential parent phases (liquid or gel) to the liquid-ordered phase appears. We therefore study systems over a wide range of temperatures focusing on those near or below the transition temperature, where the formation of crystalline phases is favored. We include temperatures relevant for yeast-based ethanol production with major applications in the wine and alternative fuel industry.

We obtained stress profiles for pure DPPC (1,2-dipalmitoyl-sn-glycero-3-phosphocholine) and mixed DPPC/ergosterol bilayers at various temperatures encompassing the liquid–gel transition using atomistic molecular dynamics simulations. We conducted 20 different, very long simulations spanning five temperatures (15, 25, 35, 45, and 50 °C) and four ergosterol concentrations (0, 10, 20, and 30 mol %, see Supporting Information for exact definitions). The lower three temperatures are below the phase transition temperature ($T_m = 41$ °C) of DPPC.[17] Although our focus is on temperatures near or below T_m, we include simulations at 50 °C for completeness and comparison with previous work. All simulations employed the NPT (1 atm) ensemble and the Gromacs 4.0.7 simulation package[18] using the 43A1-S3 force field.[19]

For details regarding the initial configuration of the systems as well as other relevant simulation parameters see Supporting Information (SI). Because of slow dynamics (mean squared displacements at lower temperatures are 10–20 times smaller in the same time range than at high temperatures, data not shown) in the gel phase and liquid-ordered systems, all
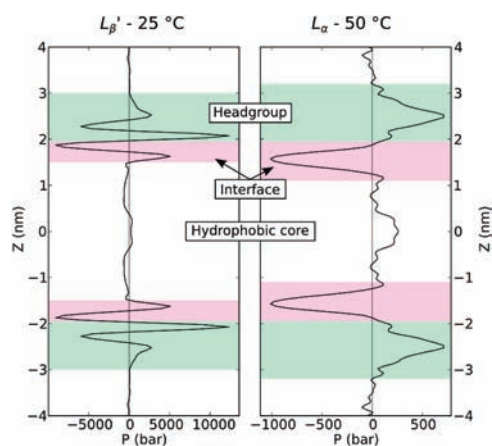
Figure 1. Stress profiles for pure DPPC bilayers in the gel phase, L_{β}' (left), and liquid disordered phase, L_{α} (right). Regions shaded in magenta show the water−hydrophobic interface. Note the different scales as the pressures in the gel phase are 5−10 times larger than those in the fluid system.
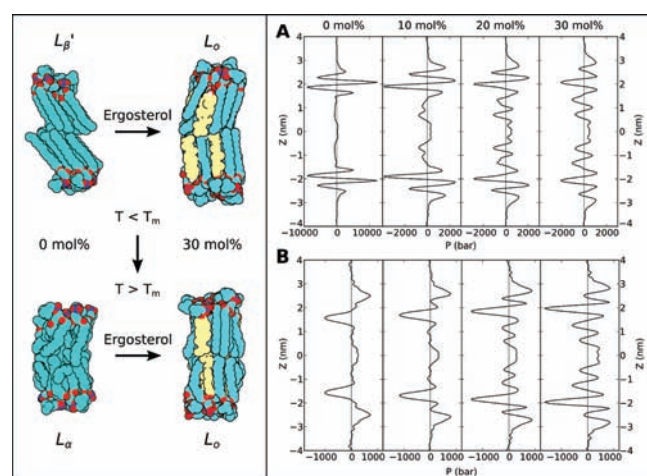

Figure 2. (Left) Selected molecules from snapshots depicting the molecular structure of the bilayers at different temperatures and changes due to addition of 30 mol % ergosterol. (Right) Stress profiles for DPPC bilayers at 25 °C (A) and 50 °C (B) containing 0−30 mol % ergosterol.

simulations were run for 400 ns to ensure that the area per molecule was equilibrated and molecules have properly sampled configurational space. The last 50 ns were used for calculation of stress profiles and other structural parameters. Although the 43A1-S3 force field was developed for lipids in fluid phases, it also reproduces very well important structural parameters of the crystalline gel phase (see Table S1 in SI for structural parameters of pure DPPC and DPPC/ergosterol obtained from our simulations including chain tilt, area/molecule, and headgroup−headgroup thickness). Stress profiles for all the simulations presented here were obtained using the method of Ollila et al.[9] (see SI) and were subject to a low-pass filter to remove high-frequency fluctuations (see Figure S1 in SI).

Stress profiles for pure DPPC in the gel phase, L_{β}', (Figure 1) are drastically different from the liquid disordered phase, L_{α}, both in shape and magnitude of the pressures. Pressures around the headgroups in the L_{β}' phase reach 12,000 bar in contrast to ∼800 bar in the L_{α} phase. Additionally, there is a single broad, positive peak in the headgroup region of the L_{α} bilayer, whereas

multiple narrow peaks are observed in the L_{β}' headgroup region. The two, large positive peaks in this region stem from the repulsive interaction of closely packed phosphate groups and glycerol-oxygen atoms as seen in density profiles (Figure S2A in SI). The water−hydrophobic interface of both systems is characterized by a large negative peak as expected from the unfavorable interaction. Lastly, the stress profile in L_{β}' is negative for most of the hydrophobic core, likely driven by attractive van der Waals interactions of the closely packed straight chains, while higher entropy of the tails in the L_{α} system leads to positive (repulsive) pressures in this region.

Structural changes after addition of ergosterol to the pure DPPC bilayers are illustrated in Figure 2. The lipid tails in the L_{β}' phase become less tilted with increasing ergosterol, as seen in the tail tilt angle distribution (Figures S3A, S4A, and S5A in SI) and increased bilayer thickness (Table S1 in SI). At 30 mol % the lipids have a significantly reduced tilt (12−13°). Ergosterol not only reduces the tilt, but it also affects the orientation (azimuthal angle, Figures S3B, S4B, and S5B in SI) of the lipids. Upon addition of ergosterol at 15 and 25 °C the tail orientation changes from a single narrow distribution to multiple broad peaks, indicating that the molecules no longer share a common orientation. This result may help explain the observation that average chain tilt of DPPC at 25 °C vanishes at low sterol concentrations.[20] Below T_m the stress profiles incur large changes even after addition of only 10 mol % ergosterol (Figures 2A and S6 and S7 in SI). This behavior agrees with the experimentally observed elimination of surface shear rigidity, unique to solid structures, at this ergosterol concentration[21] and a 50% reduction in area compressibility modulus also accompanied by elimination of surface shear rigidity observed in a similar (DMPC/12.5 mol % cholesterol) system.[22,23] The magnitude of the peak pressures around the headgroups drops by a factor of 5, and a greater number of smaller oscillating peaks begin to appear across the bilayer. At 20 and 30 mol %, the oscillating pressures become larger, especially in the hydrophobic core.

The disordered tails in the L_{α} phase become gradually more ordered and straighten with increasing ergosterol (Figure 2), which results in increased bilayer thickness (Table S1 in SI) in good agreement with X-ray diffraction results of DMPC/cholesterol systems[24] and electron density profiles of previous DPPC/ergosterol[25] and DMPC/ergosterol[26] simulations. However, in contrast to the rapid change in the gel phase once ergosterol is added, the L_{α} stress profiles (Figure 2B and S8 in SI) show a more progressive change, with the magnitude of the peak pressures around the headgroups increasing significantly only at 20 and 30 mol %. In addition, oscillatory features become extensive throughout the bilayer at 20 mol % and become pronounced at 30 mol % ergosterol. This progressive effect of ergosterol on the fluid systems compares well with experimental area compressibility moduli of fluid lipids containing cholesterol.[27] The DPPC/ergosterol stress profiles at 50 °C are in good agreement with those obtained from DPPC simulations with cholesterol[14] and other sterols[13] (see Figure S9 in SI for comparison of the 20 and 30 mol % stress profiles with previous work).

Determining the molecular origin of the oscillating peaks in the hydrophobic core due to ergosterol is not trivial as the pressures have both configurational and kinetic components. Mass density profiles of selected atoms in the 30 mol % ergosterol system (Figure S2B in SI) show that negative pressures in the hydrophobic core may be correlated with the ergosterol methyl groups. Previous simulation work by Patra[14]
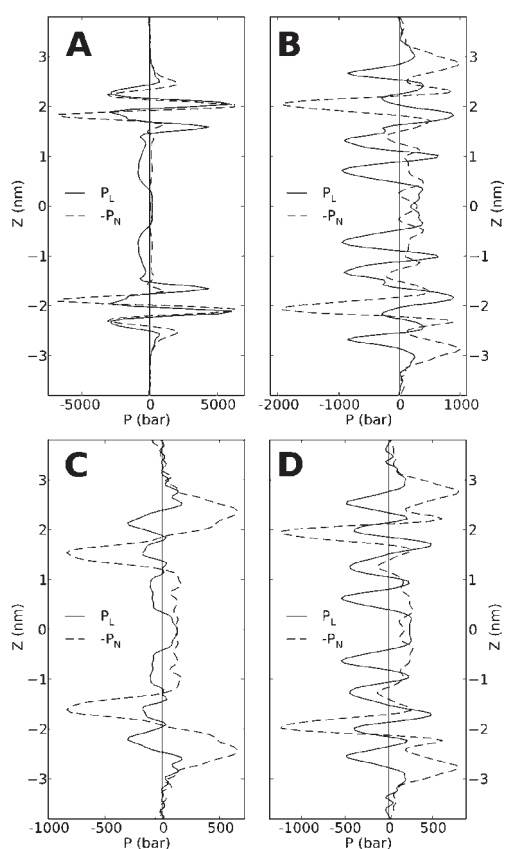
3721

dx.doi.org/10.1021/ja110327r |*J. Am. Chem. Soc.* 2011, 133, 3720–3723

Figure 3. Stress profiles separated into the lateral, P_L, and normal, P_N, components. (A) Pure DPPC at 25 °C. (B) DPPC/30 mol % ergosterol at 25 °C. (C) Pure DPPC at 50 °C and (D) DPPC/30 mol % ergosterol at 50 °C.

Figure 4. Stress profiles for DPPC bilayers with (A) 0, (B) 10, (C) 20, and (D) 30 mol % ergosterol at three temperatures below the DPPC T_m (15, 25, and 35 °C, solid lines) and two above (45 and 50 °C, dashed lines).

on DPPC/cholesterol bilayers at high temperature (50 °C) investigated the nature of these oscillating peaks in the hydrophobic core by separating the contributions from each molecule. This study showed that the oscillations directly relate to structural changes caused by the sterol, which at high temperature increases order and structure of the lipid tails. However, our stress profiles at low temperatures (Figures 1 and S6 and S7 in SI) of pure DPPC L_β' bilayers, where the tails are also highly ordered and structured, do not show these oscillations, indicating that the effect of sterols on the stress profile, and therefore the elastic properties, goes beyond simple ordering. In an attempt to resolve this, we investigate how ergosterol affects the normal, $P_N = P_{zz}$, and lateral, $P_L = (P_{xx}+P_{yy})/2$, components of the stress profile above and below T_m (Figure 3). For pure DPPC (regardless of phase) P_N is dominated by the headgroup and water−hydrophobic interface pressures, while tail interactions are more apparent in P_L (Figure 3A,C). At 30 mol % ergosterol below T_m (Figure 3B), the sterol lowers ordering of the headgroups, reducing the high pressures in this area, and uniformly redistributing the excess pressure to the tail region as observed in P_L. In the case of 30 mol % ergosterol at high temperature (above T_m, Figure 3D), local ordering of the headgroups increases P_N in this region, while P_L compensates in the tail region similarly to the lower-temperature case. Regardless of temperature, ergosterol balances the headgroup and hydrophobic core pressures as well as uniformly distributes these across the bilayer.

Comparing the stress profiles for all ergosterol concentrations across all temperatures (Figure 4) provides some insights. The
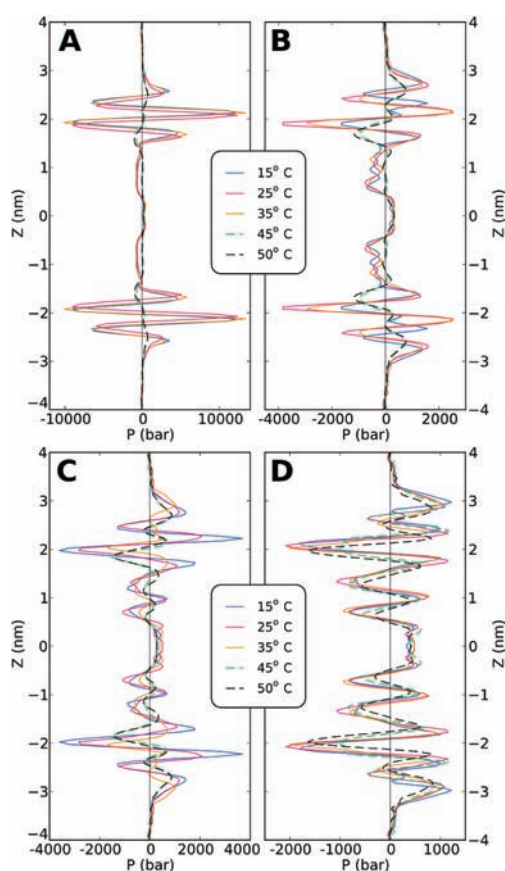
stress profiles for the L_β' DPPC at 15, 25, and 35 °C are very similar to each other, and so are the two profiles at temperatures above T_m. While we see a big change for systems below and above T_m in pure DPPC bilayers (Figure 4A), as ergosterol concentration increases (Figure 4B,C), there is a less pronounced difference below and above the T_m resulting in converging stress profiles at 30 mol % ergosterol (Figure 4D). At this ergosterol concentration the stress profiles show remarkable similarities both in shape and magnitude of the peaks across all temperatures. Although calculation of elastic properties from stress profiles is well-defined for uniform fluid systems,[16] definition and calculation of these elastic properties for crystalline and anisotropic systems below T_m are not trivial and are beyond the scope of this study (and will be presented in a follow-up publication). Nonetheless, estimates of the area compressibility modulus (K_A), bending modulus (k_c), and spontaneous curvature (c_0) at 50 °C (Table S2, SI) show very good agreement with experimental results. Similarity of the stress profiles at 30 mol % ergosterol suggests that all systems have similar mechanical moduli. The area compressibility modulus measured for DMPC/33 mol % cholesterol bilayers is nearly identical above and below T_m. Its relatively large value suggests significant strengthening of the lipid bilayer.[22,23] The similarities in the stress profiles, in conjunction with similarities in structural conformations (with differences in dynamics), indicate that the 30 mol % ergosterol systems across the 35 K temperature range are in the same liquid-ordered L_o phase in agreement with experiment.[28]

In this contribution we use stress profiles to better understand and identify the effects of sterols, here ergosterol, beyond the known fluidizing of gel phases and ordering of liquid phases. We find that the concentration dependence of these two effects is significantly different: higher ergosterol is needed to order a fluid phase than to fluidize a gel phase. With only 10 mol % ergosterol, a gel phase is effectively disrupted as seen from a decrease in tilt and a strong reduction in the headgroup region of the stress profile. With higher concentrations this effect is strengthened, but no fundamental changes are seen, indicating a threshold in ergosterol below 10 mol %. The ordering of the fluid phase on the other hand is much more gradual, and we cannot assign any threshold concentration. Interestingly the structure of the high sterol concentration (30 mol %) systems is largely temperature independent, despite differences in dynamics, indicating that they are all in the same liquid-ordered phase. By comparing the stress profiles of liquid-ordered and gel-phase membranes, we show that the effects of sterols go beyond simple ordering, but balance and uniformly distribute pressures across the bilayer. We have established that stress profiles of accurate atomistic simulations can be applied to identify different lipid phases. The difference in stress profiles between gel, ordered, and fluid phases is more severe than the difference in commonly measured quantities such as area per molecule indicating significant changes in the mechanical or rheological behavior.

In a low oxygen environment, production of sterols or unsaturated lipids is limited in microorganisms such as yeast.[29−31] Therefore, yeasts produce only saturated and mono-unsaturated lipids and rely upon ergosterol to fluidize the saturated lipids at low concentrations.[32] Ergosterol appears to fluidize saturated lipids at low concentrations by the mechanism suggested by our results—distributing the positive and negative pressures throughout the membrane rather than solely in the headgroup and interface regions. This same transition to distributed pressure takes place in fluid-phase lipids; however, it occurs gradually with concentration possibly corresponding to the larger sterol concentrations in higher organisms where there is a predominance of unsaturated lipids.[33] The significant strengthening that accompanies the pronounced distribution of lateral pressure oscillations at around 30 mol % sterol suggests that this mechanism is crucial to the well-known environmental-stress tolerance of yeasts that display higher ergosterol content (maximum ~30 mol %) in their membranes.[4]

ASSOCIATED CONTENT

Ⓢ Supporting Information. Materials and Methods section. This material is available free of charge via the Internet at http://pubs.acs.org.

AUTHOR INFORMATION

Corresponding Author
rfaller@ucdavis.edu

ACKNOWLEDGMENT

REFERENCES

(1) Meer, G.; van; Voelker, D. R.; Feigenson, G. W. *Nat. Rev. Mol. Cell Biol.* **2008**, *9*, 112–124.

(2) Schneiter, R.; Brügger, B.; Sandhoff, R.; Zellnig, G.; Leber, A.; Lampl, M.; Athenstaedt, K.; Hrastnik, C.; Eder, S.; Daum, G.; Paltauf, F.; Wieland, F. T.; Kohlwein, S. D. *J. Cell Biol.* **1999**, *146*, 741–754.

(3) Der Rest, M. E.; van; Kamminga, A. H.; Nakano, A.; Anraku, Y.; Poolman, B.; Konings, W. N. *Microbiol. Rev.* **1995**, *59*, 304–22.

(4) Bisson, L. F. *Am J. Enol. Vitic.* **1999**, *50*, 107–119.

(5) Marsh, D. *Biochim. Biophys. Acta* **2009**, *1788*, 2114–2123.

(6) Simons, K.; Vaz, W. L. C. *Annu. Rev. Biophys. Biomol. Struct.* **2004**, *33*, 269–295.

(7) Klose, C.; Ejsing, C. S.; Garcia-Saez, A. J.; Kaiser, H.-J.; Sampaio, J. L.; Surma, M. A.; Shevchenko, A.; Schwille, P.; Simons, K. *J. Biol. Chem.* **2010**, *285*, 30224–30232.

(8) Malinsky, J.; Opekarova, M.; Tanner, W. *Yeast* **2010**, *27*, 473–478.

(9) Ollila, O. H. S.; Risselada, H.; Louhivuori, M.; Lindahl, E.; Vattulainen, I.; Marrink, S. *Phys. Rev. Lett.* **2009**, *102*, 1–4.

(10) Marsh, D. *Biophys. J.* **2007**, *93*, 3884–3899.

(11) Cantor, R. S. *J. Phys. Chem. B* **1997**, *101*, 1723–1725.

(12) Lindahl, E.; Edholm, O. *J. Chem. Phys.* **2000**, *113*, 3882–3893.

(13) Ollila, O. H. S.; Róg, T.; Karttunen, M.; Vattulainen, I. *J. Struct. Biol.* **2007**, *159*, 311–323.

(14) Patra, M. *Eur. Biophys. J.* **2005**, *35*, 79–88.

(15) Gullingsrud, J.; Schulten, K. *Biophys. J.* **2004**, *86*, 3496–3509.

(16) Ben-Shaul, A. In *Handbook of Biological Physics*; Lipowsky, R., Sackman, E., Eds.; Elsevier Science: Amsterdam; New York, 1995; Vol. 1, pp 359−401.

(17) Mabrey, S.; Sturtevant, J. M. *Proc. Natl. Acad. Sci. U.S.A.* **1976**, *73*, 3862–3866.

(18) Hess, B.; Kutzner, C.; Der Spoel, D.; van; Lindahl, E. *J. Chem. Theory Comput.* **2008**, *4*, 435–447.

(19) Chiu, S.-W.; Pandit, S. A.; Scott, H. L.; Jakobsson, E. *J. Phys. Chem. B* **2009**, *113*, 27482763.

(20) Mills, T.; Huang, J.; Feigenson, G.; Nagle, J. F. *Gen. Physiol. Biophys.* **2009**, *28*, 126–139.

(21) Tierney, K. J.; Block, D. E.; Longo, M. L. *Biophys. J.* **2005**, *89*, 2481–2493.

(22) Evans, E.; Needham, D. *J. Phys. Chem.* **1987**, *91*, 4219–4228.

(23) Needham, D.; McIntosh, T. J.; Evans, E. *Biochemistry* **1988**, *27*, 4668–4673.

(24) Hung, W.-C.; Lee, M.-T.; Chen, F.-Y.; Huang, H. W. *Biophys. J.* **2007**, *92*, 3960–3967.

(25) Cournia, Z.; Ullmann, G. M.; Smith, J. C. *J. Phys. Chem. B* **2007**, *111*, 1786–1801.

(26) Czub, J.; Baginski, M. *Biophys. J.* **2006**, *90*, 2368–2382.

(27) Needham, D.; Nunn, R. S. *Biophys. J.* **1990**, *58*, 997–1009.

(28) Hsueh, Y.-W.; Gilbert, K.; Trandum, C.; Zuckermann, M.; Thewalt, J. *Biophys. J.* **2005**, *88*, 1799–1808.

(29) Mauricio, J.; Millán, C.; Ortega, J. *World J. Microbiol. Biotechnol.* **1998**, *14*, 405–410.

(30) Andreasen, A.; Stier, T. *J. Cell. Comp. Physiol.* **1954**, *43*, 271–281.

(31) Chen, L.-L.; Wang, G.-Z.; Zhang, H.-Y. *Biochem. Biophys. Res. Commun.* **2007**, *363*, 885–888.

(32) Bloch, K. E. *CRC Crit. Rev. Biochem. Mol. Biol.* **1983**, *14*, 47–92.

(33) Spector, A. A.; Yorek, M. A. *J. Lipid Res.* **1985**, *26*, 1015–35.